Journal of Applied Research and Technology

www.jart.icat.unam.mx

ICAT Instituto de Ciencias Aplicadas y Tecnología

Journal of Applied Research and Technology 24 (2026) 758-766

Original

Vapor Smoothing as a Post-Processing Technique for Enhanced Surface Finish in FDM 3D Printing

Dipak Sawant[1,2*] • Adik Yadao[1*] • Sunil Raykar[2]

[1]G H Raisoni College of Engineering and Management, Savitribai Phule Pune University, India
[2]D.Y. Patil College of Engineering and Technology, Kolhapur, Maharashtra, India

Received: 13 07 2025; Accepted: 06 10 2025
Available: 31 10 2026

Abstract: In virtue of its benefits and ability to produce intricate geometries, fused deposition modeling (FDM) is one of the most preferred additive manufacturing technologies. FDM can be used for all polymers, amongst which polylactic acid (PLA) is a widely used polymer for consumer and industrial product 3D printing. In this investigation, the analysis of vapor smoothing as a post-processing treatment to improve the surface finish of additively manufactured polylactic acid components is discussed. During the investigation, vapor smoothing is carried out for 1 mL, 2 mL, and 3 mL concentrations of ethyl acetate. Results suggest that the 3 mL concentration improves surface finish by 13.48% and 3.37% as compared to the 1 mL and 2 mL concentrations, respectively. The optimized process parameters found during this investigation are a concentration of 3 mL, a time of 180 seconds, and a layer thickness of 0.12 mm, which will lead to the highest surface finish of 3D-printed parts made with FDM.

Keywords: **Vapor smoothing, surface finish, fused deposition modeling, 3D printing.**

*Corresponding author.
E-mail address: dipaksawant0589@gmail.com (D. Sawant).
Peer Review under the responsibility of Universidad Nacional Autónoma de México.

1. Introduction

Additive Manufacturing (AM) has been around for more than 30 years and has attracted both commercial and public interest because it offers significant benefits such as printing intricate shapes all at once without the requirement for assembly. The capacity to deal with a variety of materials and the ongoing advancement of technology are the main reasons for the growth of additive manufacturing (Pérez et al., 2020; Shahrubudin et al., 2019)). AM cuts down on process time and material waste (Rajaguru et al., 2020). As shown in Figure 1, FDM prints 3D geometries by depositing material in layers with predefined thickness (Mehdiyev & Felhő, 2024). Many 3D printing techniques, including 3D plotting, stereolithography (SLA), selective laser sintering (SLS), fused deposition modeling (FDM), PolyJet modeling, and so forth, have emerged as a result of the development of additive manufacturing technology (Rahim et al., 2019). The inadequate part surface quality of FDM-made parts necessitates more research into the relationships between different process parameters and post-processing procedures (Taufik & Jain, 2022). The printed component's poor roughness makes it unusable in several applications where strong surface integrity is required. Because of this, the printed item needs to be post-processed in order to improve its surface polish, which affects its mechanical properties (Mathew et al., 2023). Everything that is done after the parts are taken out of a 3D printer is referred to as post-processing. Enhancing mechanical, chemical, and aesthetic qualities, maintaining tight tolerances, producing finishes that are nearly injection molded, and gaining more durability are all made possible by finishing and post-processing. Common post-processing methods used with fused deposition modeling (FDM) technologies include gap filling, sanding, and support removal, and enhancing thermo- mechanical qualities by annealing, UV curing, thermal exposure, and vapor smoothing is a fundamental requirement for this (Dizon et al., 2021). Optional part finishing that enhances the component's characteristics, functionality, or even appearance is a sort of secondary post-processing (Panda et al., 2020). The post-processing method for improving surface polish that uses chemical agents like ethyl acetate has been shown to be very efficient, quick, and affordable. The process yields uniform surface finishing throughout the components and doesn't need any heating devices. In this work, we monitor and optimize surface finish post-processing using vapor smoothing (Mazlan et al., 2018). Polylactic acid (PLA), a widely used biodegradable polymer in FDM, is often chosen for its ease of printing and environmental benefits. However, mechanical properties of 3D-printed parts can vary significantly based on print parameters and testing conditions (Moreno Nieto & Moreno Sánchez, 2021; Anand Kumar & Shivraj Narayan, 2018). The mechanical performance and surface quality of PLA parts can be influenced by thermal post-processing treatments (Singh et al., 2020). Parts produced using FDM often suffer from poor surface finish, visible layer lines, and limited mechanical properties, which restrict their use in high-performance applications; chemical post-processing methods such as vapor smoothing have gained attention for their ability to enhance surface properties without significant material removal (Sawant et al., 2023; Lavecchia et al., 2022). Post-processing equipment available these days helps to optimize printing and process parameters to provide customized treatments for different geometries and materials by adjusting parameters depending on the distinctive qualities of each printed product (Kantaros et al., 2024). Intelligent systems are always learning and changing, providing tailored and ideal solutions for different post-printing requirements. Future advancements in post-processing will prioritize the development of novel materials and concentrate on customized post-processing for certain materials (Fang et al., 2022). Customized abrasive media, environmentally friendly support materials, and cutting-edge surface coatings will address certain post-processing issues, guaranteeing better surface finishes, increased compatibility, and less environmental impact. Additionally, ecologically friendly solutions and sustainable methods will be given priority in post-processing going forward (Pradhan et al., 2023). However, even if automation in post-processing greatly helps, more may be done to create robotic systems that are more intelligent and flexible. The goal of research should be to develop autonomous systems that can manage complex geometries, a variety of materials, and multi-step post-processing procedures. Enhancing the accuracy and adaptability of automated post-processing will require the integration of AI-driven algorithms for adaptive control and real-time decision-making (Hossain & Lu, 2023; Keane et al., 2023). Creating industry-wide standards for post-processing procedures that guarantee uniformity, dependability, and traceability among various AM methods and materials should be the main goal of future research. Methods of qualification ought to confirm the longevity, functionality, and integrity of parts that have undergone post-processing, opening

the door for wider industrial application. The capabilities of additive manufacturing's post-processing will be improved by further research and development in these fields, opening up new opportunities for the sustainable, dependable, and efficient manufacture of high-quality components for a variety of sectors (European Commission, 2020; Chacón et al., 2017).

Now, due to technological inventions, very capable 3D printers are coming to market; even with this technology, the surface quality of additively manufactured parts sometimes has issues because of the nature of additive manufacturing, particularly in FDM; this must be addressed properly to enhance the surface finish of 3D-printed polymer parts. Due to the invention of new processing processes, this problem may be resolved. In this investigation, vapor smoothing using ethyl acetate is used as a post-processing method for improving the surface finish of 3D-printed FDM parts. From existing literature, it can be seen that the post-processing methods in 3D printing have still not been used to a large extent. Particularly, methods like vapor smoothing must be explored, as it provides excellent results from a surface finish point of view. The current investigation is carried out keeping this gap in mind. This investigation aims to study the effect of vapor smoothing on 3D-printed parts using FDM. Here, 27 parts printed using the L27 array are further post-processed using vapor smoothing by varying the concentration of solvent.

2. Experimental Analysis

For testing, an ASTM D638 Type IV standard specimen is used. The dimensions of the specimen are in mm as shown in Figure 2.

The 3D model of the specimen is prepared with SOLIDWORKS and sliced as shown in Figure 3 for 3D printing using the FlashPrint slicer. After that, the component is printed using a FlashForge 3D printer, as shown in Figure 4.

2.1 Fabrication of Specimen

FlashForge Finder with a bed size of 140 mm x 140 mm x 140 mm is used for printing the specimen. While printing, a 0.4 mm nozzle with a printing speed of 80 mm/s, 70% infill, a wall thickness of 0.8 mm, and a shell count of 2 are used. The in situ printing view is shown in Figure 4. For printing, the commercially available PLA filament from Numaker is used. The filament diameter is 1.75 mm. The printed specimens are shown in Figure 5.

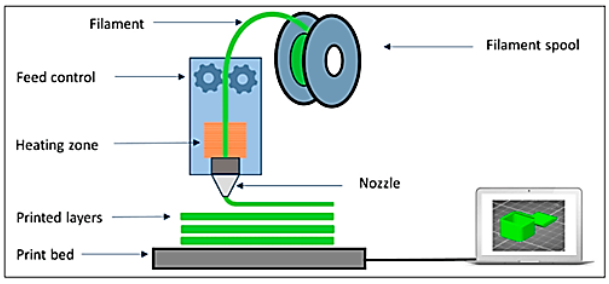


Figure 1. Schematic representation of the fused deposition modeling (FDM) 3D printing process [3].

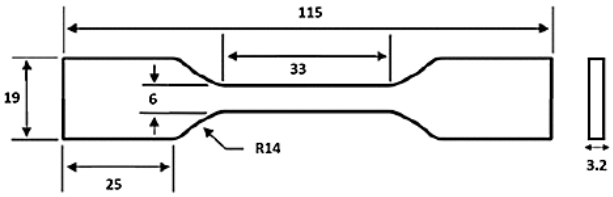


Figure 2. ASTM D638 Type IV tensile specimen (ASTM International, 2014).

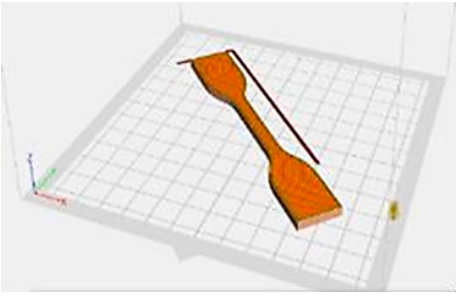


Figure 3. Slicing using the FlashPrint slicer.

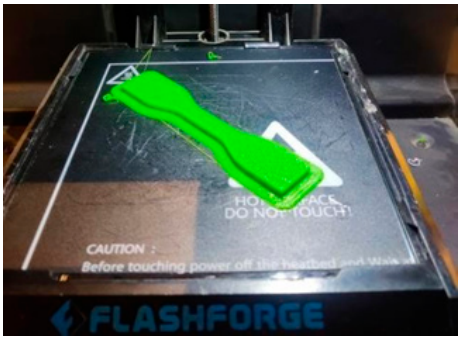


Figure 4. 3D printing of specimen on FlashForge 3D printer.

For experimental work, a Taguchi L27 array with three parameters, namely solvent concentration, exposure time, and layer thickness, is used. Of these, concentration and time are associated with vapor smoothing (post-processing), and layer thickness is associated with actual printing, since layer thickness has a significant impact on the surface finish. It is considered one of the process parameters for investigation. Each parameter is used at three levels. The parameters and their levels are shown in Table 1, and details are shown in Table 2.

Table 1. Process parameters.

Level	Concentration (mL)	Time (sec)	LT (mm)
1	1	140	0.12
2	2	160	0.14
3	3	180	0.16

2.2 Surface Roughness Measurement

After printing, the surface roughness of 3D-printed parts is measured with a Japan-made Miyutoyo SJ-210 handy surface roughness tester, as shown in Figure 6. While measuring, the tester is set to a probe speed of 0.5 mm/s, a cutoff length of 0.8 mm, and 5 intervals. Surface roughness is measured at each of the three points. Three repetitions are taken. The surface measurements are shown in Table 2.

Vapor smoothing is done using a 500 mL glass container holding the precise amount of ethyl acetate (1 mL, 2mL, 3mL) and a steel container filled with water. To avoid direct contact between the specimen and the liquid solvent, each specimen was positioned and hung in the center of the container using an MS wire that was suspended from the top of the glass container lid by a screw, as shown in Figure 7. After that, the container was submerged in 100 °C boiling water to allow the solvent to evaporate during the course of the treatment.

3. Results and Discussions

For the analysis of data on surface roughness, AOM plots, a response table, ANOVA, and contour plots are used. From the response table of means, it can be clearly seen that the delta value for layer thickness is 0.6410, which is the maximum among the other process parameters, i.e., concentration of solvent and exposure time; therefore, layer thickness has the highest impact on Ra. This is obvious as layer thickness defines surface roughness because it is actually the height of the layer that is deposited during printing.

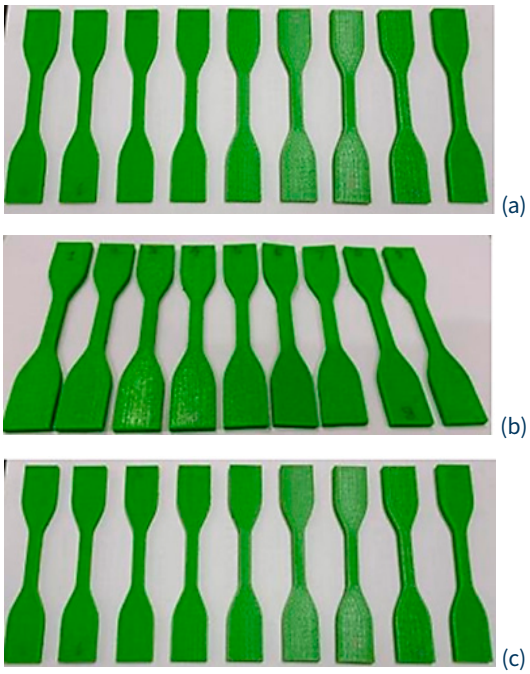


Figure 5. 3D-printed specimens for different concentrations: (a) specimens for 1 mL concentration, (b) specimens for 2 mL concentration, and (c) specimens for 3 mL concentration.



Figure 6. Surface roughness measurement using a Mitutoyo surface roughness tester.



Figure 7. Vapor smoothing process using ethyl acetate solvent.

Table 2. Surface roughness readings after post-processing treatment.

Concentration (ml)	Time (s)	Layer Thickness (mm)	Roughness Ra (µm)	Predicted value of Ra	% error
1	140	0.12	1.031	0.9522	7.643
1	140	0.14	1.131	1.2726	12.51
1	140	0.16	1.601	1.593	0.499
1	160	0.12	1.05	0.9262	11.79
1	160	0.14	1.239	1.2466	0.613
1	160	0.16	1.631	1.567	3.923
1	180	0.12	0.922	0.9002	2.364
1	180	0.14	1.176	1.2206	3.792
1	180	0.16	1.588	1.541	2.959
2	140	0.12	0.911	0.867	4.829
2	140	0.14	1.021	1.1874	16.29
2	140	0.16	1.523	1.5078	0.998
2	160	0.12	0.92	0.841	8.586
2	160	0.14	1.019	1.1614	13.97
2	160	0.16	1.551	1.4818	4.461
2	180	0.12	0.8	0.815	1.875
2	180	0.14	0.956	1.1354	18.76
2	180	0.16	1.478	1.4558	1.502
3	140	0.12	0.837	0.7818	6.594
3	140	0.14	0.998	1.1022	10.44
3	140	0.16	1.511	1.4226	5.85
3	160	0.12	0.835	0.7558	9.485
3	160	0.14	1.001	1.0762	7.512
3	160	0.16	1.478	1.3966	5.507
3	180	0.12	0.759	0.7298	3.847
3	180	0.14	0.944	1.0502	11.25
3	180	0.16	1.473	1.3706	6.951

Table 3. Response table for means.

Level	Concentration (ml)	Time (s)	LT (mm)
1	1.2632	1.1738	0.8961
2	1.1310	1.1916	1.0539
3	1.0929	1.1218	1.5371
Delta	0.1703	0.0698	0.6410
Rank	2	3	1

But during vapor smoothing, concentration has a high impact on Ra, with a delta value of 0.1703, and time has the least impact, with the lowest delta value, which is 0.0698. When the concentration of solvent is increased up to 3 mL, a sufficient amount of solvent vapor becomes available to interact with the surface of the 3D-printed polymer part, which makes the surface smoother; but at a lower concentration, i.e., up to 1 mL, a limited amount of solvent vapor is available for interaction with the surface of the part, which does not improve the roughness to a greater extent.

This trend is visible in AOM plots, which also indicate a decrease in surface roughness from 1 mL to 3 mL. That is, the surface becomes smoother with an increase in

solvent concentration. From the mean values of the AOM plot, the minimum roughness is found at a 3 mL concentration, which is 1.0928 µm. The increase in roughness at a 2 mL concentration, as compared to a 3 mL concentration, is 3.37%. The increase in roughness at a 1 mL concentration, as compared to a 1mL concentration, is 13.48%. The increase in roughness at a 1 mL concentration, as compared to a 2 mL concentration, is 10.46%. But higher concentrations may cause softening of the part, which may lead to warping of the part. Also, this may lead to structural failures. Due to vapor smoothing, the surface of 3D-printed components becomes semi-hot (does not cause any melting), which tends to soften the surface, causing surface irregularities to merge into one another; this reduces the stepping effect and makes the surface smooth. This is also known as layer line diffusion, which is the main reason for getting superior surface finish in vapor smoothing.

For the exposure time, the minimum roughness is found at a 180 s cycle time, which is 1.1217 µm. The increase in roughness at a 160 s cycle time, compared to a 180 s cycle time, is 5.85%. The increase in roughness at a 140 s cycle time, compared to a 180 s cycle time, is 4.43%.

The increase in the roughness at a 160 s cycle time, as compared to a 140 s cycle time, is 1.49%.

The minimum roughness is found at a 0.12 mm layer thickness, which is 0.8961 µm. The increase in the roughness at a 0.14 mm layer thickness, as compared to a 0.12 mm layer thickness, is 14.96%. The increase in the roughness at a 0.16 mm layer thickness, as compared to a 0.12 mm layer thickness, is 41.70%. The increase in the roughness at a 0.16 mm layer thickness, as compared to a 0.14 mm layer thickness, is 31.44%.

Table 4. Analysis of variance.

Source	DF	Adj SS	Adj MS	F-Value	P-Value
Regression	3	1.99169	0.66390	73.62	0.000
Concentration	1	0.13056	0.13056	14.48	0.001
Time	1	0.01217	0.01217	1.35	0.257
LT	1	1.84896	1.84896	205.04	0.000
Error	23	0.20741	0.00902		
Total	26	2.19910			
R sq (pred)	R-sq	R-sq (adj)	R-		
0.0949616	90.57%	89.34%			
87.58%					

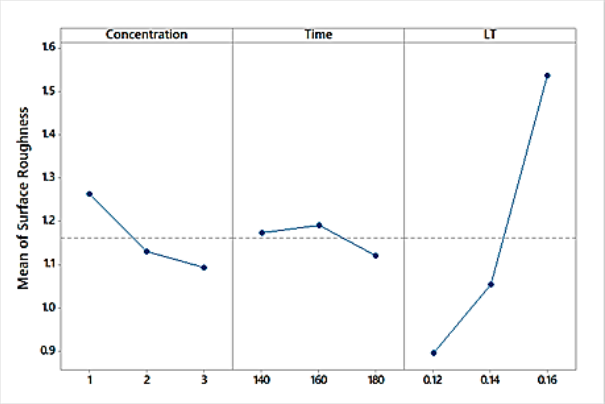


Figure 8. AOM plot for surface roughness.

From regression-based ANOVA, it can be seen that the p-value for concentration is 0.001. Therefore, as far as vapor smoothing is concerned, concentration affects Ra at the 95% confidence level, as the p-value is less than 0.05. But exposure time does not have a noteworthy effect on it at the 95% confidence level, as the p-value is 0.257. The regression model has an R^2 value of 90.57%, an adjusted R^2 value of 89.34%, and a predicted R^2 value of 87.58%. Hence, this model explains 90.57% of the variation in roughness data, and the prediction model explains 87.58% of the variation in Ra value. So, the model shows a good fit as far as analysis is concerned. As shown in Figure 8, all the profiles are contained within +/-20 µm, which are the extreme limits of the surface roughness profile. In those samples, the roughness profiles of samples 19, 20, and 21 are well within limits, and the average heights of peaks to valleys are comparatively smaller as compared to other samples. For samples 1, 2, and 3, the average heights of peaks to valleys are on the higher side. These results are visible in AOM plots also.

From the regression model, it can be seen that layer thickness has the highest impact, followed by solvent concentration and exposure time, which was already discussed in the previous section. A close fit is observed between the predicted and actual data. This can be observed from the percentage error, which varies between 0.6% and 11% (and is 18% for only one experiment). The predicted values and percentage errors are shown in Table 2.

$$\begin{aligned} Roughness\ Ra = &- 0.703 \\ &- 0.0852\ Concetration \\ &- 0.00130\ Time + 16.02\ LT \end{aligned} \quad (1)$$

To find out the working range of process parameters for vapor smoothing, a contour plot is drawn for Ra; it is shown in Figure 9. It can predict the working range of concentration and time for better Ra results.

Here, for the lightest green color, Ra is < 0.8, and for lighter and light green, surface roughness is in the range of 0.8 to 1 and 1 to 1.2, respectively. For darker shades of green, it is more than 1.2 µm. From the contour plot, the working range of solvent concentration is more than 1.5% to 3% with a combination of exposure time between 140 and 180 s. To find the optimal setting of process parameters for better results of surface roughness, a desirability function is used, and the optimal plot is drawn using the Response Optimizer in Minitab. Since minimization of surface roughness is the goal of optimization, the minimized setting and minimization equation are used to optimize the process parameters. These equations are described below.

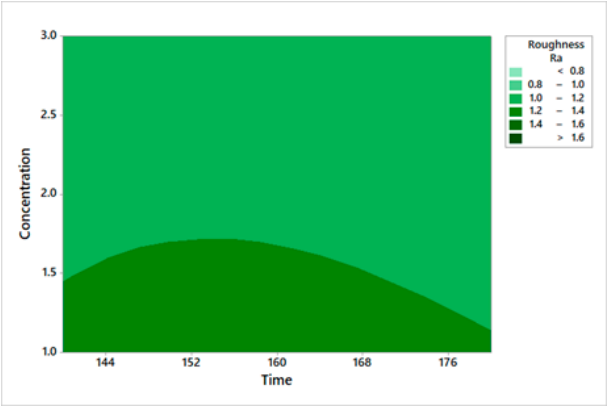


Figure 9. Contour plots for surface roughness.

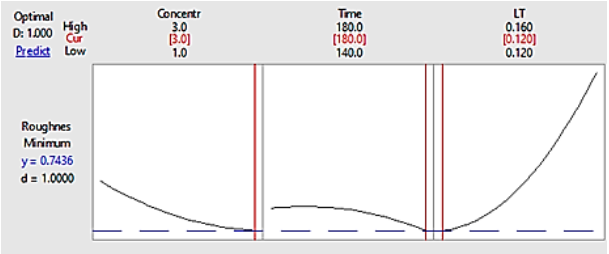


Figure 10. Response optimizer plot for surface roughness.

$$d_i = 0 \quad i > U_i \tag{2}$$

$$d_i = [(U_i - i)/(U_i - T_i)]^{ri} \quad T_i < i < U_i \tag{3}$$

$$d_i = 1 \quad i < T_i \tag{4}$$

where:

i = predicted value of i^{th} response
T_i = target value for i^{th} response
L_i = lowest acceptable value for i^{th} response
U_i = highest acceptable value for i^{th} response
D_i = desirability for i^{th} response
D = composite desirability
r_i = weight of desirability function of i^{th} response

From the response optimizer shown in Figure 10, the predicted optimum settings are found to be a concentration of 3 mL, an exposure time of 180 s, and a layer thickness of 0.12 mm as the optimum process parameters. For these parameters, the desirability is found to be 1, and the predicted surface roughness is 0.7436 µm.

To validate the results of prediction, three trial tests were conducted with the predicted optimum process parameters. The results are: for specimen 1, the roughness is 0.7439; for specimen 2, the roughness is 0.7439; and for specimen 3, the roughness is 0.7411. Hence, very few errors are found in the actual and predicted roughness from the Response Optimizer. Therefore, the Response Optimizer with desirability is a suitable technique for optimization in manufacturing scenarios.

4. Comparison of Vapor Smoothing with Disc Polishing and Sanding

For the purpose of comparison, a few samples are prepared with different 3D printing parameters as shown in Table 5. After 3D printing of these samples, they are post-processed with vapor smoothing, sanding, and disc polishing, and then the surface finish is measured for these samples. It can be seen from the table that there is an improvement in surface finish with vapor smoothing compared to disc polishing. Therefore, vapor smoothing has a clear edge over disc polishing and sanding as a post-processing technique.

Table 5. Comparison table for vapor smoothing with disc polishing and sanding.

3D Printing Parameters			s/f before post-processing (Ra)	s/f after post processing (Ra)			% Improvement of VS vs DP	% Improvement of VS vs S
LT	PS	In %		VS	DP	S		
0.12	80	70	3.161	1.031	1.985	2.538	48.06	59.37
0.14	90	80	3.014	1.133	1.965	2.631	42.34	56.93
0.16	100	75	3.434	1.143	2.019	2.531	43.38	54.83

where:

s/f = surface finish (Ra)
LT = layer thickness in mm
PS = printing speed in mm/s
In % = infill %
VS = vapor smoothing
DP = disc polishing
S = sanding

5. Conclusions

The current investigation is focused on vapor smoothing as a post-processing method for FDM-based 3D printing. The following are some key findings from the investigation:

1. Solvent concentration has a high impact on surface finish. It is found that a 3 mL concentration improves surface finish by 13.48% and 3.37% as compared to the 1 mL and 2 mL ethyl acetate concentrations, respectively.
2. From the response table, it is observed that the solvent concentration has a higher impact and it is ranked as 1, with a delta value of 0.1703, and time has the least impact, with a delta value of 0.0698.
3. The regression model suggests a good fit between predefined values and experimental values, with an R-sq of 90.57% and an R-sq of predicted values of 87.58%. Also, the error between regression and actual values ranges from 0.6% to 11%.
4. The optimum process parameters are 3 mL of concentration, an exposure time of 180 s, and a layer thickness of 0.12 mm

Conflict of interest

The authors have no conflict of interest to declare.

Funding

The authors received no specific funding for this work.

Acknowledgements

The authors are grateful for the support for this research provided by D.Y. Patil College of Engineering & Technology, where the experiments were conducted in its laboratories.

References

Anand Kumar, S., & Shivraj Narayan, Y. (2018). Tensile testing and evaluation of 3D-printed PLA specimens as per ASTM D638 type IV standard. In *Innovative Design, Analysis and Development Practices in Aerospace and Automotive Engineering (I-DAD 2018) Volume 2* (pp. 79-95). Singapore: Springer Singapore.
https://doi.org/10.1007/978-981-13-2718-6_9

ASTM International. (2014). Standard test method for tensile properties of plastics. ASTM international

Chacón, J. M., Caminero, M. A., García-Plaza, E., & Núnez, P. J. (2017). Additive manufacturing of PLA structures using fused deposition modelling: Effect of process parameters on mechanical properties and their optimal selection. *Materials & Design*, *124*, 143-157.
https://doi.org/10.1016/j.matdes.2017.03.065

Dizon, J. R. C., Gache, C. C. L., Cascolan, H. M. S., Cancino, L. T., & Advincula, R. C. (2021). Post-processing of 3D-printed polymers. *Technologies*, *9*(3), 61.
https://doi.org/10.3390/technologies9030061

European Commission. (2020). Conformity assessment procedures for 3D printing and 3D printed products to be used in a medical context for COVID-19.
https://health.ec.europa.eu/document/download/000cf966-c81e-41d7-a452-1b2d4ce17230_en?filename=md_mdcg_qa_3d_ppp_covid-19_en.pdf

Fang, Q., Xiong, G., Zhou, M., Tamir, T. S., Yan, C. B., Wu, H., ... & Wang, F. Y. (2022). Process monitoring, diagnosis and control of additive manufacturing. *IEEE Transactions on Automation Science and Engineering*, *21*(1), 1041-1067. https://doi.org/10.1109/TASE.2022.3215258

Hossain, S. S., & Lu, K. (2023). Recent progress of alumina ceramics by direct ink writing: Ink design, printing and post-processing. *Ceramics International*, *49*(7), 10199-10212. https://doi.org/10.1016/j.ceramint.2023.01.143

Kantaros, A., Ganetsos, T., Petrescu, F. I. T., Ungureanu, L. M., & Munteanu, I. S. (2024). Post-production finishing processes utilized in 3D printing technologies. *Processes*, *12*(3), 595. https://doi.org/10.3390/pr12030595

Keane, G., Healy, A., & Devine, D. (2023). Post-processing methods for 3D printed biopolymers. In *Additive Manufacturing of Biopolymers* (pp. 229-264). Elsevier. https://doi.org/10.1016/B978-0-323-95151-7.00006-5

Lavecchia, F., Guerra, M. G., & Galantucci, L. M. (2022). Chemical vapor treatment to improve surface finish of 3D printed polylactic acid (PLA) parts realized by fused filament fabrication. *Progress in Additive Manufacturing*, *7*(1), 65-75. https://doi.org/10.1007/s40964-021-00213-2

Mathew, A., Kishore, S. R., Tomy, A. T., Sugavaneswaran, M., Scholz, S. G., Elkaseer, A., ... & John Rajan, A. (2023). Vapour polishing of fused deposition modelling (FDM) parts: a critical review of different techniques, and subsequent surface finish and mechanical properties of the post-processed 3D-printed parts. *Progress in Additive Manufacturing*, *8*(6), 1161-1178. https://doi.org/10.1007/s40964-022-00391-7

Mazlan, S. N. H., Alkahari, M. R., Ramli, F. R., Maidin, N. A., Sudin, M. N., & Zolkaply, A. R. (2018). Surface finish and mechanical properties of FDM part after blow cold vapor treatment. *J. Adv. Res. Fluid Mech. Therm. Sci*, *48*(2). https://www.akademiabaru.com/doc/ARFMTSV48_N2_P148_155.pdf

Mehdiyev, Z., & Felhő, C. (2024). Enhancing Properties of 3D Printed Polymers: A Review of Recent Post Processing Methods. *International Journal of Advanced Natural Sciences and Engineering Researches*, *7*(10), 411–417. https://www.as-proceeding.com/index.php/ijanser/article/view/2115

Moreno Nieto, D., & Moreno Sánchez, D. (2021). Design for additive manufacturing: tool review and a case study. *Applied Sciences*, *11*(4), 1571. https://doi.org/10.3390/app11041571

Panda, S. S., Chabra, R., Kapil, S., & Patel, V. (2020). Chemical vapour treatment for enhancing the surface finish of PLA object produced by fused deposition method using the Taguchi optimization method: SS Panda et al. *SN Applied Sciences*, *2*(5), 916. https://doi.org/10.1007/s42452-020-2740-1

Pérez, M., Carou, D., Rubio, E. M., & Teti, R. (2020). Current advances in additive manufacturing. *Procedia Cirp*, *88*, 439-444. https://doi.org/10.1016/j.procir.2020.05.076

Pradhan, S. R., Singh, R., & Banwait, S. S. (2023). 3D printing assisted investment casting of dental crowns for recycling of DMLS waste. *Arabian Journal for Science and Engineering*, *48*(3), 3289-3299. https://doi.org/10.1007/s13369-022-07155-z

Rahim, T. N. A. T., Abdullah, A. M., & Md Akil, H. (2019). Recent developments in fused deposition modeling-based 3D printing of polymers and their composites. *Polymer Reviews*, *59*(4), 589-624. https://doi.org/10.1080/15583724.2019.1597883

Rajaguru, K., Karthikeyan, T., & Vijayan, V. (2020). Additive manufacturing–State of art. *Materials today: proceedings*, *21*, 628-633. https://doi.org/10.1016/j.matpr.2019.06.728

Sawant, D. A., Shinde, B. M., & Raykar, S. J. (2023). Post processing techniques used to improve the quality of 3D printed parts using FDM: State of art review and experimental work. *Materials Today: Proceedings*. https://doi.org/10.1016/j.matpr.2023.09.202

Shahrubudin, N., Lee, T. C., & Ramlan, R. J. P. M. (2019). An overview on 3D printing technology: Technological, materials, and applications. *Procedia manufacturing*, *35*, 1286-1296. https://doi.org/10.1016/j.promfg.2019.06.089

Singh, S., Rajeshkannan, A., Feroz, S., & Jeevanantham, A. K. (2020). Effect of normalizing on the tensile strength, shrinkage and surface roughness of PLA plastic. *Materials Today: Proceedings*, *24*, 1174-1182. https://doi.org/10.1016/j.matpr.2020.04.431

Taufik, M., & Jain, P. K. (2022). Part surface quality improvement studies in fused deposition modelling process: a review. *Australian Journal of Mechanical Engineering*, *20*(2), 527-551. https://doi.org/10.1080/14484846.2020.1723342